

Browse ▾

My Settings ▾

Get Help ▾

Subscribe

All ▾

Enter keywords or phrases (Note: Searches metadata only by default. A search for 'smart grid' = 'smart AND grid')



Search within Publication

Advanced Search

Other Search Options ▾

Browse Conferences > Progress in Electromagnetic Re... > 2018 Progress in Electromagnet... ?

Progress in Electromagnetic Research Symposium (PIERS)

Copy Persistent Link

Browse Title List

Sign up for Conference Alerts

Proceedings

All Proceedings

Popular

2018 Progress in Electromagnetics Research Symposium (PIERS-Toyama)

DOI: 10.23919/PIERS-Toyama43567.2018

Search within results



Per Page: 25 ▾

Export ▾

Email Selected Results ▾

Showing 1-25 of 472

Refine

Author ▾

Affiliation ▾

Select All on Page

Sort By: Sequence ▾

2018 Progress In Electromagnetics Research Symposium (PIERS | Toyama)

Publication Year: 2018, Page(s): 1 - 1

Abstract (158 Kb)



2018 Progress In Electromagnetics Research Symposium (PIERS | Toyama)

Publication Year: 2018 Page(s): 1 - 1



Need Full-Text

access to IEEE Xplore for your organization

Feedback

2018 Progress In Electromagnetics Research Symposium (PIERS — Toyama)

Copyright and Reprint Permission

© 2018 The Institute of Electronics, Information and Communication Engineer (IEICE). Personal use of this material is permitted. However, permission to reprint/republish this material for advertising or promotional purposes or for creating new collective works for resale or redistribution to servers or lists, or to reuse any copyrighted component of this work in other works must be obtained from the IEICE. As copyright holder for the PIERS 2018 Toyama Proceedings (abstracts and full-length papers), the IEICE grants the IEEE the nonexclusive, irrevocable, royalty-free worldwide rights to publish, sell, and distribute the copyrighted work for the Conference named above and any content derived from the copyrighted work in any format or media without restriction.

IEEE Catalog Number: CFP18C18-ART
ISBN: 978-4-88552-315-1 C3855

THE ELECTROMAGNETICS ACADEMY

The Progress in Electromagnetics Research Symposium (PIERS) is sponsored by The Electromagnetics Academy.

The Electromagnetics Academy is devoted to academic excellence and the advancement of research and relevant applications of the electromagnetic theory and to promoting educational objectives of the electromagnetics profession. PIERS provides an international forum for reporting progress and advances in the modern development of electromagnetic theory and its new and exciting applications.

Founded by the late Professor Jin Au Kong (1942–2008) of MIT in 1989, The Electromagnetics Academy is a non-profit organization registered in USA.

PIERS Founding Chair:

Jin Au Kong, MIT, USA

President of The Electromagnetics Academy:

Professor Leung Tsang, University of Michigan, USA

JOURNAL: PROGRESS IN ELECTROMAGNETICS RESEARCH

Progress In Electromagnetics Research (PIER) publishes peer-reviewed original and comprehensive articles on all aspects of electromagnetic theory and applications. This is an open access, on-line journal PIER (E-ISSN 1559-8985). It has been first published as a monograph series on Electromagnetic Waves (ISSN 1070-4698) in 1989. It is freely available to all readers via the Internet.

PIER is a non-profit organization.

WWW.JPIER.ORG

Contact Email: work@jpier.org

Founding Editor in Chief:

Jin Au Kong, MIT, USA

Editors in Chief:

Professor Weng Cho Chew, University of Illinois at Urbana-Champaign, USA

Professor Sailing He, Royal Institute of Technology, SWEDEN; JORCEP, Zhejiang University, CHINA

Progress In Electromagnetics Research Symposium
August 1–4, 2018
Toyama, JAPAN

PIERS 2018 TOYAMA ORGANIZATION

PIERS Chair

Leung Tsang, University of Michigan

PIERS 2018 Toyama General Chair

Kazuya Kobayashi, Chuo University

PIERS 2018 Toyama General Co-chairs

Weng Cho Chew, Purdue University

Sailing He, Royal Institute of Technology; JORCEP, Zhejiang University

Tsuneki Yamasaki, Nihon University

**PIERS 2018 Toyama Technical Program Committee Chair
and Co-Chairs**

Kazuya Kobayashi, Chuo University (Chair)

Ivan Andronov, St. Petersburg State University (Co-Chair)

Iam-Choon Khoo, The Pennsylvania State University (Co-Chair)

Qing Huo Liu, Duke University (Co-Chair)

Tadao Nagatsuma, Osaka University (Co-Chair)

Yoichi Okuno, South China Normal University; Kumamoto University (Co-Chair)

Motoyuki Sato, Tohoku University (Co-Chair)

Yury Shestopalov, University of Gävle (Co-Chair)

Ari Sihvola, Aalto University (Co-Chair)

Meisong Tong, Tongji University (Co-Chair)

Jan Vrba, Czech Technical University in Prague (Co-Chair)

Contents

Measurement and Modeling of Multi-frequency Microwave Emission of Soil Freezing and Thawing Processes	31
Z-R Relationships for Weather Radar in Indonesia from the Particle Size and Velocity (Parsivel) Optical Disdrometer	37
Imaging Plasma Inhomogeneities Using Spatial Wave Field Processing with DWFT Approximation ...	42
Optimal Cavities to Enhance Free-space Matching in Solar Cells	48
Parabolic Equation of Diffraction Theory: Why It Works Better than Expected?	53
Dipole Field Diffraction by a Strongly Elongated Spheroid in High-frequency Approximation	59
Diffraction of TM Polarized EM Waves by a Nonlinear Inhomogeneous Dielectric Cylinder	66
Measurement of the Diffraction Coefficient of a Trihedral Cone with Homogeneous Neumann Boundary Conditions	71
Heterogeneously Integrated Optoelectronic Devices for Implantable Neural Interfaces	78
A High-speed Pipelined ADC Based on Open-loop Amplification	82
A Chip of Pulse-laser-assisted Dual-beam Fiber-optic Trap	86
Rotation of a Trapped Microsphere in a Misaligned Dual-beam Optical Tweezer	92
Linear Cellularization Enabling Millimeter-wave Train Radio Communication Systems in 5G Era	99
Improvement in Accuracy of Breakpoint Distance Model for Path Loss Prediction	107
Effects of Storm Attenuation over Satellite Links in Sub-tropical Africa	115
A Comparative Study of Dual-slope Path Loss Model in Various Indoor Environments at 14 to 22 GHz	121
An Empirical Approach to Omnidirectional Path Loss and Line-of-sight Probability Models at 18 GHz for 5G Networks	129
The Second Order Moment Equation of Crossly Polarized EM-waves Due to Depolarization in Propagation through Continuous Isotropic Random Medium	137
Guided-mode Resonance in Waveguide Cavity	144
Microwave Interstitial Applicator Array for Treatment of Pancreatic Cancer	150
Microwaves in Medical Diagnostics and Treatment	155
Numerical Study of Stroke Detection Using UWB Radar	160
Prediction of Cement-based Materials' Water Content with the Use of Electromagnetic Homogenisation Schemes	164
Radar Bistatic Configuration for Soil Moisture Estimation at L-band Using Global Sensitivity Analysis Method	169
Two-slab High Sensitivity Technique for Measurement of Permittivity of a Dielectric Slab in a Rectangular Waveguide	176
Shape Measurement Based on Combined Reduced Phase Dual-directional Illumination Digital Holography and Speckle Displacements	184
A- Φ Formulation Time Domain Integral Equations Free from Interior Resonances	190
MOD Based Discontinuous Galerkin PMCHW Method for Simulating Transient Scattering Characteristics of Dielectric Objects	197

Fast Solution of Volume Integral Equations Based on Meshless Discretization	203
Analyzing Phased Arrays with Basis Functions Associated with Characteristic Modes	208
FDTD Analysis of Radiation and Reflection of Electromagnetic Fields in Finite Length Microstrip Lines with Terminal Cross-section	213
Uncertainties in EMC — Calibration and Testing	220
3D Holographic Display with Enlarged Field of View Based on Binary Optical Elements	227
Hydrophone Based on a Fiber Bragg Grating	233
Exploration of Optical Amplifiers Based on Erbium (Er^{3+}) and Ytterbium (Yb^{3+}) Doped Fiber Segments and Its Emerging Applications	237
Deep Learning for Interference Cancellation in Non-orthogonal Signal Based Optical Communication Systems	241
On-chip Detection from Directly Modulated Quantum Dot Microring Lasers on Si	249
Silicon-based Polarization Analyzer by Polarization-frequency Mapping	254
Optoelectronic Frequency Conversion Employing an Electro-absorption Modulated Laser for a Cube Satellite Earth Station	257
High SHF Band RF Signal Relay Employing Radio over Multi-mode Fibers	262
Modelling Defects on Junction between Coaxial Cables in View of Fault Diagnostic	266
Surface Electromagnetic Waves Propagation Guided by Dissipative Dielectric Material Sandwich between Two Periodic Multilayered Isotropic Materials in Prism Coupled Configuration	274
Modified Wang Shaped Ultra-wideband (UWB) Fractal Patch Antenna for Millimetre-wave Applications	280
Combined Electric and Magnetic Field Tuning of the Impedance of Lanthanum Strontium Manganite Thin Film Interdigital Electrode Devices	285
Magnetization State Determination Using Deep Learning	291
Ultra-broadband Tungsten Absorber	297
A Refined VR Based Video Indirect Ophthalmoscope	301
Fundamental Study for Optical Transillumination Imaging of Arteriovenous Fistula — System Integration into Practical Compact Device for Bedside Application	308
Monitoring of Nanopowder Combustion Ignited by Laser Radiation	311
Effect of Microwave Radiation on the Thermal Properties of the Electroexplosive Copper Nanopowder	317
Application of Laser-speckle Correlation Method for Blood Coagulation Estimation	320
The Development of a High Sensitive Micro Size Magnetic Sensor Named as GSR Sensor Excited by GHz Pulse Current	324
Engineering of GMI Effect of Fe-rich Microwires by Stress Annealing	332
Optimization of GMI Effect and Magnetic Properties of Co-rich Microwires by Joule Heating	338
Numerical Estimation Based on Ray Tracing for Automotive Radar Beam Through Curved Dielectric Slab	344
Electric Field Strength in Layered Materials with Varied Parameters	347
On the Evaluation of Sources in Highly Accurate Time Domain Simulations on the Basis of Faber Polynomials	352
Extension of the Parabolic Equation Method in the Time Domain	357
A Fast Algorithm for Electromagnetic Scattering from One-dimensional Dielectric Rough Surface	362
SRCNN-based Enhanced Imaging for Low Frequency Radar	366
An Improved Algorithm for Enhancing Fingerprint Image Quality	371
A High-speed Data Acquisition and Preprocessing Method for Wirelessly Supervising Train Braking System	376

Characteristic Parameter Estimation of Chipless RFID Signals Based on USRP	381
NDF and On-axis Resolution of an Axicon in Near Zone: Numerical Experiments	386
On the Number of Independent Equations in Phase Retrieval Problem: Numerical Results in Circular Case	392
Programmable Pulse Processor Using Cascaded Microrings on Silicon Photonic Circuits	396
WT-based Data-length-variation Technique for Fast Heart Rate Detection	399
Transmission Line Analogy for Wave Propagation in Graphene-based Structures	405
Emulating Tunneling with Elastic Vibrating Beams	410
Design of RFID Tag Antenna Based on the Cole-Cole Model of Human Abdomen	414
Characteristics of 340 GHz Slow Wave Structure for Staggered Double-vane Traveling Wave Tube	420
Design and Modeling of Tunable Band-stop Filter Using Evanescent Mode Resonators	424
An Example of Notch Filter Design Spec for the IM Noise Signal Cancellation in 800 MHz CDMA Frequency Band	428
Influence of Tropospheric Ducts on Radio Propagation over Sea Surface	432
Mode Absorption Filters Based on Graphene-on-silicon Waveguides	437
Optical Force for Particle Trapping in a Nanobeam Photonic Crystal Cavity	440
Analysis of Interferogram Phase Noise by Bi-static Data Sets of TerraSAR-X	444
Modified Helical Coils Structure for Uniform Magnetic Flux Density	449
A Low-profile Antenna Design for LTE/WWAN Smartphone Application	454
Eutrophication Analysis of Water Reservoirs by Remote Sensing and Neural Networks	458
Filtered Back Projection and Simultaneous Algebraic Reconstruction Technique for Image Formation on Square-shaped Physical Phantom Aimed at Microwave Imaging Applications	464
Estimation of the Energy Characteristics of a Multi-position Radar System for the Control of Small-sized Space Debris for Various Orbital Zones	470
Estimation of the Resolution of a Multi-position Radar for the Control of Small-sized Space Debris Objects That Are Not Resolved by Angular Coordinates	476
Efficient Electromagnetic Scattering Analysis for Multi-scale Problems Using Green's Functions of Arbitrary Scatterers	482
Plasmonic Properties of Electrolytes beyond Classical Nanophotonics — A Two-fluid, Hydrodynamic Approach to Nonlocal Soft Plasmonics	490
Modeling the Magnetic Field Radiated from a Ferrite Rod Antenna for Mining Proximity Detection Systems	496
A Novel Approach to Microfabrication of Planar Microstrip Meander-line Slow Wave Structures for Millimeter-Band TWT	506
Radiation Pattern Inspection of the FMCW Signal Using Asynchronous Electro-optic Measurement System	510
Novel Measurement Set-ups of FTB Stress Propagation in an IC	513
Speed of Light in Vacuum in the Case of a Lumped Electric Circuit	520
Numerical Models of a Multilayered Graphene Structure	527
Algorithms to Detect and Localize the Source of a Wideband Pulse Signal	533
A Numerical Analysis of a Periodic Resonant Structure at THz Frequencies	537
Vision-based and Differential Global Positioning System to Ensure Precise Autonomous Landing of UAVs	542
High Frequency Scattering from Conducting Rectangular Cylinder via Surface Equivalence Theorem ..	547
<i>H</i> -polarized Plane Wave Diffraction by Thick Conducting Slits	553

An Enhanced Model for the Analysis of Non-uniform Multiconductor Transmission Lines Based on Scattering Theory	559
Spatial Prediction of Electromagnetic Fields Using Few Measurements	565
Coupling of Differential and Common Modes of Two-line Circuits in the Multi-conductor Transmission-line Theory Including Radiation	570
Orbital Angular Momentum Generation Using Composite Quasi-continuous Metasurfaces with Perfect Efficiency	575
Giant Nonlinear Response of Subwavelength Dielectric Resonators Enhanced by Bound States in the Continuum	580
Metasurfaces for Improvement Magnetic Resonance Imaging Characteristics: Novel Designs and In Vivo Studies	585
Characterization of Terahertz Plasmonic Structures Based on Metallic Wire Woven Meshes	588
Helicity-induced Multifunctional Devices Based on Hybrid Metasurfaces	592
Integrated Circuits Using Photonic-crystal Slab Waveguides and Resonant Tunneling Diodes for Terahertz Communication	599
Improved Detection Strategies for Nonlinear Frequency-division Multiplexing	606
Open Area Concealed Weapon Detection Sensor System Development	611
Design and Analysis of Inductive Reluctance Position Sensor	621
Wireless Energy Harvesting in RFID Applications at 5.8 GHz ISM Band, a System Analysis	627
A Novel Microwave Applicator for Sandy Soil Disinfection	636
Study of Simultaneous Switching Noise in Two-dimensional Transport Theory including Radiation Effect	642
Effect of Absorbing Coating on Shielding Effectiveness of Electromagnetic Shielding Fabric	648
Optimal Design of Yagi Microstrip Antenna Based on Particle Swarm Optimization with Fitness Estimation	653
Analysis of Singular-point Generating Mechanisms Based on the Correlations among the Parameters in Coherency Matrix and Those in the Optimized Scattering-mechanism Vector in PolInSAR	661
Imaging Performance of Backward and Forward Bistatic SAR	669
Adaptive Subsurface Visualization System Using Phase Retrieval Method and Complex-valued Self-organizing Map	677
Influence Analysis of Uneven Surface on Landmine Detection Using Holographic Radar	683
A 3.5–8 GHz Analog Complex Cross-correlator for Interferometric Passive Millimeter-wave Security Imaging Systems	692
Shuffled Structure for 4.225 GHz Antireflective Plates: A Proposal Proven by Numerical Simulation ...	700
A Modified Method for Measuring the Faraday Rotation Angle	706
Data Augmentation Using Conditional GANs for Facial Emotion Recognition	710
An Efficient Face Recognition Algorithm Based on Deep Learning for Unmanned Supermarket	715
Efficient Data Record System for Radio Backend	719
Pre-processing VDIF Data in FPGA	723
A Novel Extraction Method for Melodic Features from MIDI Files Based on Probabilistic Graphical Models	729
Model Calculations for Hardware Correlator at SHAO	734
Waveguide BPF Composed of Dielectric Frequency Selective Structure with High Suppression of Spurious Mode	739
Design Optimization of RF-MEMS Based Multiband Reconfigurable Antenna Using Response Surface Methodology	743

Indoor Localization System Using Commensal Radar Principle	751
An Improved Successive-cancellation Decoding Algorithm for Polar Code Based on FPGA	756
Improved Electromagnetic Compatibility Design for Printed Circuit Board of Automobile Atmosphere Lamp	760
Next Approach of HEMS WPT	765
Numerical Study of Hyperthermia Applicator System for Tumor Treatment in Head and Neck Region	770
An Interference EMG Model of Selected Water Samples	775
Algorithms for Flying Object Detection	782
Formation of Ray Trajectories of HF Radiowaves in Midlatitude and Highlatitude Ionosphere during Halloween Storm 2003 According to Radiotomography Data	787
Multiple-bounce Modeling of High-rise Buildings with Airborne Tomography Array	791
The Study of Composite Scattering from the Target over a Randomly Rough Surface Using SAR/ISAR Imaging	797
Scattering Characteristics of Vortex Electromagnetic Waves for a Wedge	801
Application of the RK4IP Method for the Numerical Study of Noise-like Pulses in Supercontinuum Generation	805
Numerical Analysis of Chaotic Dynamics Produced in a Photonic Crystal Fibers	810
Classification and Properties of Modes in Bragg Fibers	814
Inverse Synthetic Aperture Ladar Imaging Algorithm for Space Maneuvering Target Using Synchrosqueezing Short-time Fourier Transform	819
Analysis of Spectrum Properties of Integrated Optical Chips Applied on IFOG	827
Semi Circular Printed Monopole Antenna with U Shaped Slot for UWB Applications	833
Design of 5 Way Wide Band Wilkinson Power Divider for 6 to 18 GHz Applications	838
Magneto-optical Properties of a Magnetic Fluid in the THz Frequency Range	843
Multiband Circularly Polarized Synthetic Aperture Radar (CP-SAR) Onboard Microsatellite Constellation	848
Comparison Design of X-band Microstrip Antenna for SAR Application	854
Gain Enhancement of C Band Linearly-polarized Microstrip Antenna with Square Parasitic Patch for Airborne LP-SAR Sensor	858
Dual-band Circularly-polarized Microstrip Antenna for Nano Satellite	864
3D Printed Wideband Circularly Polarized Pyramidal Horn Antenna	868
Unidirectional Radiation and Gain Enhancement of Circularly Polarized Printed Slot Antenna by Several Shapes of Reflector	872
An 8-channels FPGA-based Reconfigurable Chirp Generator for Multi-band Full Polarimetric Airborne/Spaceborne CP-SAR	876
An PC-based Airborne SAR Baseband System	882
Numerical Solution for Received Power Estimation in a Wave Propagation — A Case of Ground Based C-band SAR Test	889
Indoor Experiment of SAR Interferometry with 79 GHz MIMO Sensor	894
Single Post-event PolSAR Data Based Earthquake/Tsunami Damage Information Extraction in Urban Areas	899
Interferometry Synthetic Aperture Radar (InSAR) Application for Flood Area Detection Observed by Sentinel 1A	905
Multi-temporal Land Deformation Monitoring in V Shape Area Using Quasi-Persistent Scatterer (Q-PS) Interferometry Technique	910

Interferometry Synthetic Aperture Radar (InSAR) Application for Flood Area Detection Observed by Sentinel 1A

Pakhrur Razi^{1,2}, J. T. S Sumantyo², Fajar Febriany¹,
 Mohammad Nasucha², and Jamrud Aminuddin²

¹Physics Department, Universitas Negeri Padang, Sumatra 25131, Indonesia

²Center for Environmental Remote Sensing, Chiba University, Chiba 236-8522, Japan

Abstract— Almost every year, flood and landslide occur at Pangkalan Lima Puluh Kota district, West Sumatra, Indonesia. These not only destroyed the agricultural but also isolated the area. The area is essential for supporting transportation connection in the center of Sumatra. However, the handling of this issues is insufficient then scientific information is a necessity. In this research, flood monitoring data extracted using InSAR processed by SNAP Sentinel-1 toolbox. The data were provided by European Space Agency (ESA) Ground Range Detected (GRD) High-resolution, Interferometric Wide Sentinel-1A observation product in ascending and descending orbit Both co-polarization VV and cross-polarization VH of satellites detected slightly different flood covered. The cross-polarization is high sensitive than co-polarization. The result was the present great potential of SAR satellite data for detection and delimitation flood risk in the area.

1. INTRODUCTION

Flooding disaster event occurred in the most area in the world. Even in some country the tragedy has been natural phenomena in the rainy season. The flood is not only the destroyed the environmental but also in social and economic impact because the disaster is obstructing people's livelihood, break the transportation routes then the area become isolated. So, the fact requires more attention from local authorities in managing in before, during and after the geo-hazard occurrence.

In recent year, the number of disasters attacks Pangkalan Koto Baru, West Sumatra, Indonesia. Flood is one of the common tragedy that has a long history in the area. In last three-year, large-scale flooding event occurrence on November 2015, February 2016, March 3, 2017. The trend of flooding occurs at the end of the year (Oct.–Dec.) until early month on next year (Jan.–Mar.) regularly [1], because of rainfall intensity is high during the time [2]. Then the local government by BPBD (Regional Disaster Management Agency) has categorized the area into middle-high land movement and flooding [3].

For mitigation and evaluation of flood event, the Synthetic Aperture Radar (SAR) interferometry data has used to extract the information about the surface area. The data obtained from SAR satellite operation that emits the electromagnetic wave to the earth and receive its reflection [4]. The satellite can acquire data without preventing by a cloud during day and night time [5]. Then the earth surface feature can be observed correctly with high image resolution. In this case, Sentinel-1A satellite data that provided by European Space Agency (ESA) was used to extract the flood information. The data acquisition is February 20, 2017, and March 4, 2017, for before and during the inundate event respectively.

Mapping the areas that affected by flood and property damage is crucial for evaluating and preventing probability the flood disaster coming in future. In this work, we discuss the application of interferometry C-band SAR data for mapping the flood area in Pangkalan Koto Baru using Sentinel-1A images.

2. AREA OF STUDY AND SATELLITE DATASET

The study area located at 0.10°N, 100.76°E Pangkalan Koto Baru, Lima Puluh Kota district West Sumatra Indonesia. The zone is the main road connecting West Sumatra province and Riau province. This way is essential as the trade lane from both region that more than ten thousand [6] vehicle in this way every day. However, the area has a longtime history of flooding, even every year at least onetime flood occurred notice since 2011. Recently, the last large-scale flood occurred on March 3, 2017. Besides destroyed the agriculture and infrastructure also triggering the landslide in some zone. The area has high rainfall intensity along the year [1], in particular, at the end until the early month of the next year with the intensity is more than 300 mm/month [2].

Figure 1 shows the area of research on Pangkalan Koto Baru, which the red square is inhabitant area and white square is a basin that has been a control water level in the field. The most of

the field is mountainous that have valleys between them which have been inhabitant area. In the valleys passed some rivers that sometimes overflow then inundate the resident zone.

For investigation flood area and damage analyze, the Sentinel-1A (C-band) SAR data with Ground Range Detected (GRD) product format used. The mode of satellite data is Interferometric Wide (IW) with has swath width area 250 km and has a dual polarization ($VV + VH$). The GRD range-azimuth resolution is 20×22 m with pixel spacing 10×10 m [7]. The acquisition date is March 4, 2017, February 20, 2017, at 11.32 am for flood event and waterbodies respectively.

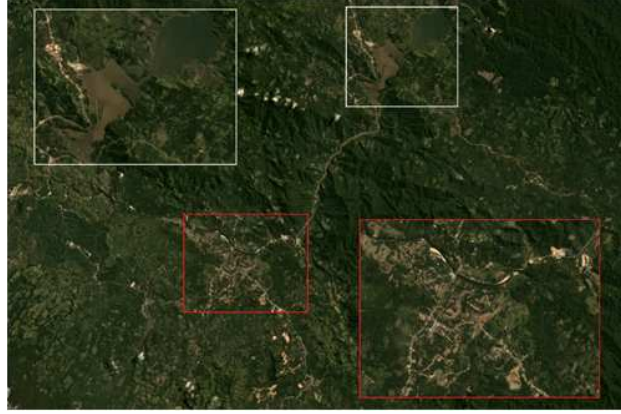


Figure 1: The study area of flooding on Pangkalan Koto Baru, West Sumatra, Indonesia. The red square is settlements area; the white square is a basin. The image captured by Sentinel-2A in July 2017.

Table 1: Satellite Sentinel-1A dataset with dual polarization ($VV + VH$) and azimuth range resolution 20×22 m.

Satellite data	Beam Mode	Type	Acquisition	Track	Orbit
S1A	IW	GRD	04-Mar.-2017	69	15541
S1A	IW	GRD	20-Feb.-2017	69	15366

3. METHODOLOGY

SAR interferometry is a technique that develops to extract information from a pair of SAR images in different time acquisition [8]. The SAR data achieved by emitting an electromagnetic wave to the earth surface with a specific frequency. The lowest frequency has high sensitivity [9] to surface feature with an accuracy of the topography and displacement in meter and millimeter respectively [10].

Flood area can be analyzed by its backscatter coefficient σ^0 [11], which has the low value than others because the satellite signal reflected away from the sensor then the area look dark in SAR images. The processing flow is shown in Figure 2.

4. RESULT AND DISCUSSION

In flood investigation, we use two satellite data, before and during the event. The data in before flood event was used to mapping the water body on the area, and comparing with flood event. To extracted water bodies and flood area information, the backscatter coefficient threshold was applied to separate water and non-water. To decide the value, statistical analyze was applied by selecting the water area. The water class, which has lowvalue backscatter coefficient than other. Furthermore, to verify the value, the histogram analyzing also was considered. The backscatter coefficient value for water is shown in Figure 3.

In Figure 3, the minimum and maximum value of the backscatter coefficient for 6022 pixels sample were selected in both basin area (B1, B2) of 0.001 and 0.0251 respectively. The coefficient value > 0.0251 correspond to land area. In this case, the time acquisition of the satellite data is in 12-hour flooding then some field less identified. Based on amplitude value for copolarization (VV) and cross-polarization (VH) the area of the study depicted in Figure 4.

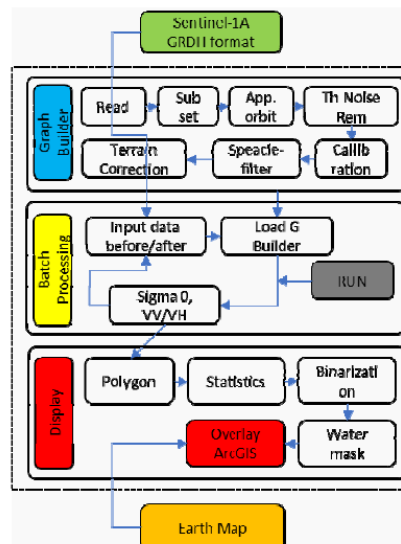


Figure 2: Flood area investigation processing flow based on SNAP software developed by ESA.

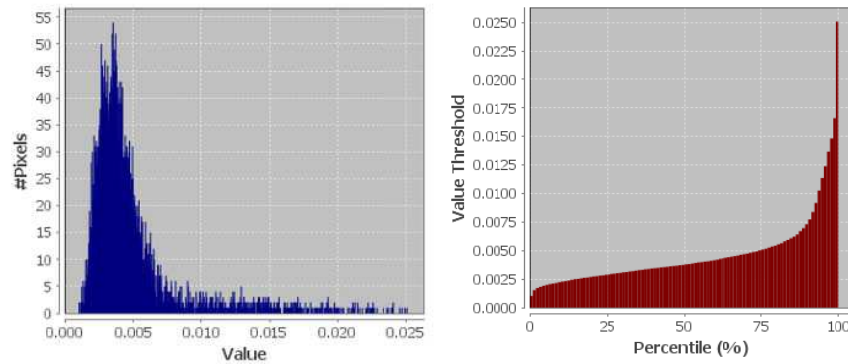


Figure 3: Statistical value of flood water backscatter coefficient for the 6022-pixel sample in Pangkalan Koto Baru basin, West Sumatra Indonesia.

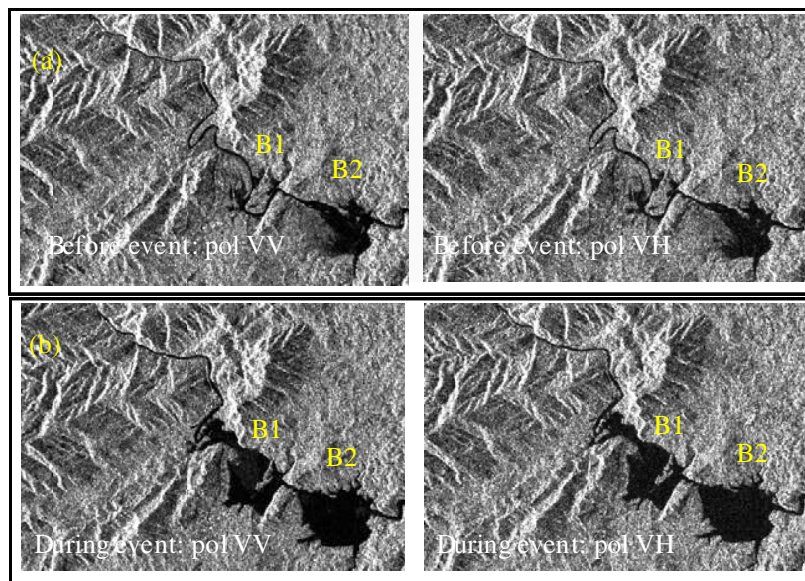


Figure 4: Images based on the amplitude value of the study area for co-polarization (VV) and cross-polarization (VH) observation. (a) SAR image before flood event (20-02-2017), (b) SAR image during flood event (04-03-2017).

Figure 4 shows the images based on the amplitude value in the study area, that observed by Sentinel-1A with co-polarization (VV) and cross-polarization (VH) before and during flooding. In basin (B1) has the land area in the center. Also basin (B2) has a half area approximately filled with water in before the event that observed by both polarization (Figure 4(a)). Whereas, during the flooding both of basin has a vast area that inundated with water (Figure 4(b)).

Figure 5 shows inundated area on Pangkalan Koto Baru, from two zones as a sample. In both sample are Pangkalan Koto Baru basin and Pangkalan Sub-district center. The water bodies filled up with a yellow color and the inundated area is blue and green observed by VV and VH polarization respectively. For equal backscatter coefficient threshold value, cross-polarization VH observation has more inundated area than co-polarization VV .

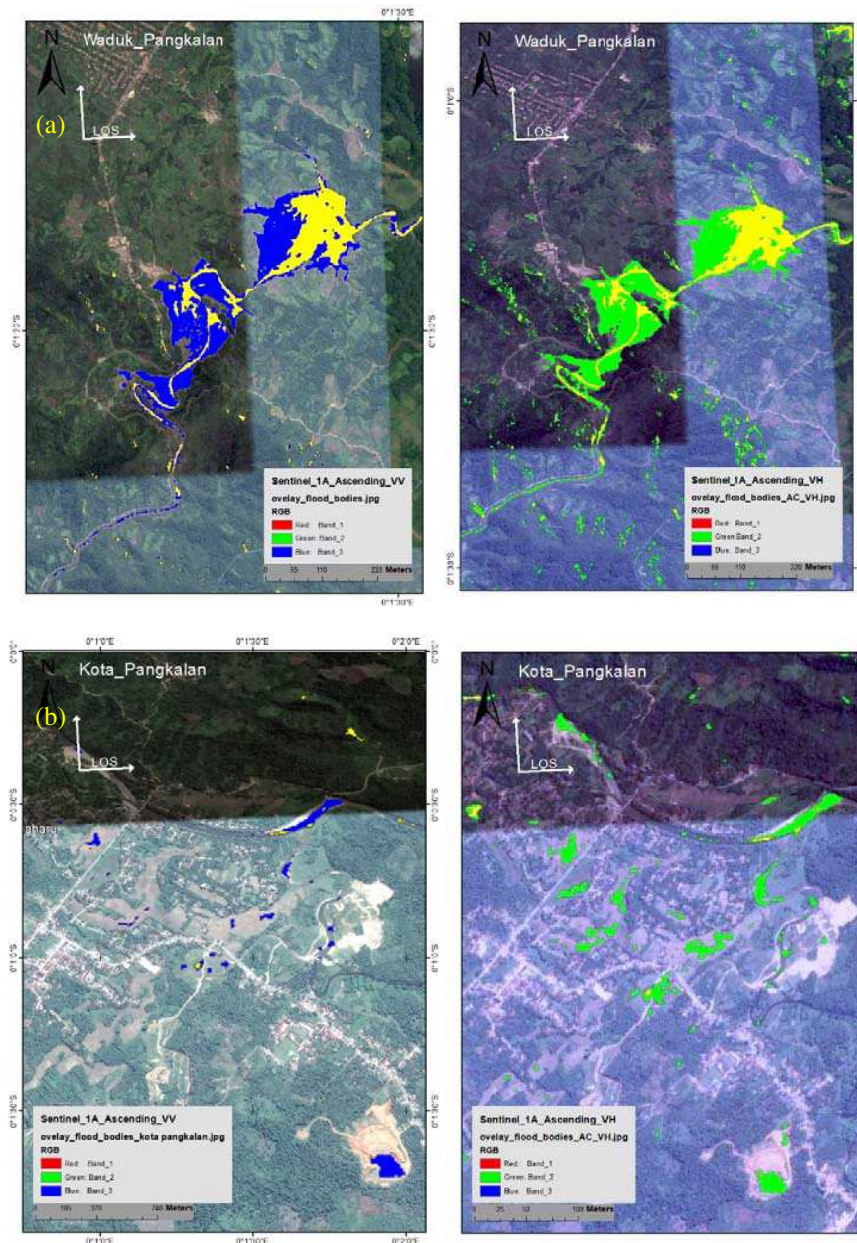


Figure 5: Overlay the flood area and the water bodies for two sample, observed by co-polarization (VV) and cross-polarization (VH): (a) Pangkalan Koto Baru basin, (b) Pangkalan Sub-district center.

5. CONCLUSION

This paper presents the capabilities of interferometry remote sensing data processed by SNAP software for detecting and managing the flooding area in Pangkalan Koto Baru. Inhabitant area, the flood is less identified because of the acquisition time of SAR data observed after 12-hour

flooding. However, in the two basins, the inundated area is clearly observed. Interferometry SAR observation with Co-polarization VV is less sensitive to flood detection than cross-polarization VH on the area.

ACKNOWLEDGMENT

The authors would like to thank Chiba University Excellent International Student Scholarship, KEMENRISTEK DIKTI, Universitas Negeri Padang, ESA Europe, JAXA Japan, NASA, BNPB, BPBD, BMKG-SUMBAR.

REFERENCES

1. Razi, P., J. Tetuko, S. Sumantyo, D. Perissin, and A. Munir, “Persistent scattering interferometry SAR based velocity and acceleration analysis of land deformation: Case study on kelok sembilan bridge,” *TSSA IEEE Conf.*, 9–12, 2017.
2. BMKG, “Rainfall intensity,” 2014–2018, [Online] Available: http://dataonline.bmkg.go.id/mcstation_metadata, Accessed: Jan. 20, 2018.
3. BPBD, “Wilayah daerah rawan bencana tsunami, gempa dan cuaca ekstrim (longsor dan banjir) di provinsi sumatera barat tahun 2016,” [Online] Available: http://bpbd.sumbarprov.go.id/images/2017-07-11-1499763282-Daerah_Rawan_Bencana_Pergerakan_Tanah_dan_Banjir_2016.pdf, Accessed: Apr. 30, 2018.
4. Kampes, B. M., *Radar Interferometry*, Vol. 12, Springer, The Netherlands, 2006.
5. Ketelaar, V. B. H. G., *Satellite Radar Interferometry: Subsidence Monitoring Techniques*, Springer, The Netherlands, 2009.
6. Razi, P., et al., “3D land mapping and land deformation monitoring using persistent scatterer interferometry (PSI) ALOS PALSAR: Validated by geodetic GPS and UAV,” *IEEE Access*, Vol. 6, No. 1, 12395–12404, 2018.
7. ESA, “Interferometric wide swath,” Esa 2000–2018, [Online] Available: <https://sentinel.esa.int/web/sentinel/user-guides/sentinel-1-sar/acquisition-modes/interferometric-wide-swath>.
8. Ferretti, A., *Satellite InSAR Data Reservoir Monitoring from Space*, EAGE, Netherlands, 2014.
9. Refice, A., et al., “SAR and InSAR for flood monitoring: Examples with COSMO-SkyMed data,” Vol. 7, No. 7, 2711–2722, 2014.
10. Perissin, D. and F. Rocca, “High-accuracy urban DEM using permanent scatterers,” *IEEE Trans. Geosci. Remote Sens.*, Vol. 44, No. 11, 3338–3347, 2006.
11. Pulvirenti, L., M. Chini, S. Member, N. Pierdicca, S. Member, and G. Boni, “Use of SAR data for detecting floodwater in urban and agricultural areas: The role of the interferometric coherence,” Vol. 54, No. 3, 1532–1544, 2016.



公益財団法人

電気通信普及財団

The Telecommunications Advancement Foundation



公益財団法人

Toyama Convention Bureau

富山コンベンションビューロー



Japan National
Tourism Organization



公益財団法人 村田学術振興財団

The Murata Science Foundation

